J. Cell. Mol. Med. Vol 12, No 1, 2008 pp. 241-257

Phosphorylated PP2A (tyrosine 307) is associated with Alzheimer neurofibrillary pathology

R. Liu [a, f] , X.-W. Zhou [a, f] , H. Tanila [b] , C. Bjorkdahl [a] , J.-Z.Wang [c] , Z.-Z. Guan [d] , Y. Cao [d] , J.-Å. Gustafsson [e] , B. Winblad [a] , J.-J. Pei [a]

[a] Karolinska Institutet, KI-Alzheimer Disease Research Center (KI-ADRC), Novum, Huddinge, Sweden
[b] Department of Neurobiology, A. I. Virtanen Institute, Kuopio, Finland
[c] Department of Pathophysiology, Tongji Medical College, Huazhong University of Science and Technology, Wuhan, PR China
[d] Department of Pathology and Molecular Biology, Guiyang Medical College, PR China
[e] Department of Biosciences and Nutrition, Karolinska Institutetet, NOVUM, Stockholm, Sweden
[f] Department of Pathophysiology, Tongji Medical College, Huazhong University of Science and Technology, Wuhan, PR China

Received: November 20, 2007; Accepted: January 17, 2008

Abstract

Down-regulation of protein phosphatase 2A (PP2A) is thought to play a critical role in tau hyperphosphorylation in Alzheimer's disease (AD). *In vitro* phosphorylation of PP2A catalytic subunit at Y307 efficiently inactivates PP2A. A specific antibody against phosphorylated (p) PP2A (Y307) (PP2Ac-Yp307) was used to investigate possible PP2A down-regulation by known pathophysiological changes associated with AD, such as Aβ accumulation and oestrogen deficiency. Immunohistochemistry and immunofluorescence confocal microscopy showed an aberrant accumulation of PP2Ac-Yp307 in neurons that bear pre-tangles or tangles in the susceptible brain regions, such as the entorhinal cortical cortex and the hippocampus. Experimentally, increased PP2Ac-Yp307 was observed in mouse N2a neuroblastoma cells that stably express the human amyloid precursor protein with Swedish mutation (APPswe) compared with wild-type, and in the brains of transgenic APPswe/ presenilin (PS1, A246E) mice, which corresponded to the increased tau phosphorylation. Treating N2a cells with Aβ25-35 mimicked the changes of PP2Ac-Yp307 and tau phosphorylation in N2a APPswe cells. Knockout of oestrogen receptor (ER) α or ERβ gave similar changes of PP2Ac-Yp307 level and tau phosphorylation in the mouse brain. Taken together, these findings suggest that increased PP2A phosphorylation (Y307) can be mediated by Aβ deposition or oestrogen deficiency in the AD brain, and consequently compromise dephosphorylation of abnormally hyperphosphorylated tau, and lead to neurofibrillary tangle formation.

Keywords: Aβ • oestrogen receptor • PP2A phosphorylation (Y307) • tau phosphorylation • Alzheimer's disease

Introduction

Protein phosphatase 2A (PP2A) is one of the most important serine/threonine phosphatases in mammalian brains. Its activity is determined by the holoenzyme composition (scaffolding/structural A, regulatory/targeting B and catalytic C subunits), PP2A inhibitors [1] and post-translational modifications of the catalytic subunit [2, 3]. Decreases of PP2A activity [4], PP2A mRNA level [5], and a major PP2A heterotrimer enzyme $AB_{\alpha}C$ [6] have been reported in the Alzheimer's disease (AD) brain. It is also established

*Correspondence to: Jin-Jing PEI, MD., Ph.D., Karolinska Institutet, KI-Alzheimer Disease Research Center (KI-ADRC), Novum Plan 5, Novum, S-14157, Huddinge, Sweden.
Tel.: +46 85 85 83 64 9; Fax: +46 85 85 83 88 0
E-mail: Jin-Jing.Pei@ki.se

doi: 10.1111/j.1582-4934.2008.00249.x

that inhibition of PP2A leads to tau hyperphosphorylation at several sites, such as the PHF-1 sites seen in the AD brain [7, 8]. In addition, tau hyperphosphorylation has been observed in transgenic mice with a dominant negative mutant form of the catalytic subunit of PP2A [9]. Down-regulation of PP2A carboxyl methylation at the L309 site might be the underlying mechanism hampering the heterotrimer formation [3, 10]. Alternatively, phosphorylation of the PP2A catalytic subunit at the Y307 site by receptor and non-receptor protein tyrosine kinases can inactivate PP2A [11–13].

The majority (~70%) of clinically diagnosed sporadic AD cases have a large number of extracellular senile plaques (SPs), consisting of amyloid β-peptide (Aβ), and intracellular neurofibrillary tangles (NFTs), consisting of abnormally hyperphosphorylated tau as paired helical filaments (PHF-tau) [14]. Previous *in vivo* studies have demonstrated that a high level of Aβ increases brain tau pathologies in transgenic mice carrying the APP Swedish mutation (APPswe) with a tau mutation (P301L) [15], in P301L tau transgenic mice injected with Aβ42 fibrils [16], and in triple-transgenic mice harbouring presenilin-1 (PS1, M146V), APPswe and tau (P301L) mutations [17]. However, the relationship between Aβ deposition and PHF-tau in AD brains remains largely elusive. Similarly to Aβ accumulation, oestrogen deficiency is capable of activating several tau kinases, such as protein kinase B (PKB/Akt), glycogen synthase kinase-3 (GSK-3), mitogen-activated protein kinases (MAPKs): p38, extracellular signal-regulated kinase (ERK) and c-Jun N-terminal kinase/stress-activated protein kinase (JNK/SAPK) [18–25]. By up-regulating these kinases, oestrogen deficiency may cause tau hyperphosphorylation [14] and promote NFT formation. In contrast, much less is known about the effects of Aβ accumulation and oestrogen deficiency on the main negative regulator of tau kinases, PP2A [7, 26–28].

To address the mechanism of reduced PP2A activity in AD brain and the consequent effect on tau phosphorylation, the present study investigated level and distribution of inactive/phosphorylated (p) PP2A (Y307) (PP2Ac-Yp307) in relationship to tau phosphorylation in AD brain samples and several experimental models. The effect of Aβ was tested *in vitro* in mouse N2a neuroblastoma stably expressing the human amyloid precursor protein with Swedish mutation (APPswe) and wild-type (WT) cell lines exposed to Ab25-35, and *in vivo* in the brains of transgenic APPswe/ presenilin (PS1, A246E) mice. Oestrogen deficiency was mimicked by selective knockout of ERα or ERβ receptors in mice. We found a consistent increase in the levels of PP2Ac-Yp307 in parallel with tau hyperphosphorylation in all these models.

Materials and methods

Materials

For all primary antibodies used in this study, see details in Table 1. Aβ25-35 and purified PTP1B were bought from Sigma-Aldrich (Stockholm, Sweden). Blocking peptide to phospho-PP2A (Y307) was purchased from Santa Cruz Biotechnology (Santa Cruz, CA, USA). Cytosolic abnormally hyperphosphorylated tau (AD p-tau) and PHF-tau were isolated from AD brains [29].

In this study, 10% formalin-fixed tissue blocks of the medial temporal lobe from six neuropathologically confirmed AD cases and two controls, including the entorhinal, hippocampal and temporal cortices, and/or amygdala for immunohistochemistry were obtained from Huddinge Brain Bank (Table 2). Fresh frozen ventral cortical tissue samples from brains of seven transgenic APPswe/PS1 (A246E) [30, 31] and seven non-transgenic 16-month-old female mice were prepared as previously described [32]. Fresh brains (five each from 9-month-old WT, ER$\alpha^{-/-}$ and ER$\beta^{-/-}$ female mice [33, 34]) were dissected after putting animals into deep sleep by intraperitoneal injection of sodium pentobarbital (60 mg/g) (Department of Biosciences and Nutrition, Karolinska Institutet, Novum, Sweden).

Cell culture and cell treatment

Wild-type N2a cells and APPswe N2a cells were grown in six-well culture plates (60 mm-diameter) to 70–80% confluence in complete media (Dulbecco's modified Eagle's medium, Dulbecco's Modified Eagle's Medium (DMEM)/ Opti-minimum essential medium, MEM [1:1]; 5% foetal bovine serum (FBS), 1% penicillin/streptomycin [PEST] and 0.2% Fungizone [GIBCO, Invitrogen, Stockholm, Sweden]), then the cells were switched to media with 0.5% FBS for 24 hrs. The cells were treated with 1 μM sodium butyrate for 12 hrs with or without further treatment of 25 μM Ab25-35 in 0.5% FBS growth medium for 0, 4, 12 or 24 hrs. Prior to Aβ25-35 treatment, 1 mM stock solution was prepared in double-distilled H_2O and maintained for 3 days at room temperature to allow polymerization [35].

Table 1 Antibodies used in the study

Antibodies	Epitopes	Dilution	References and sources
4G8	Human Aβ17-26 (within APP)	1/500	Biosource
pPP2A (Y307, poly)	PY307 (inactive form)	1/100	Santa Cruz
R123d (poly)	PP2A C subunit (aa 299-309)	1/1000	Reference 37
Anti-PP2A Cα(mAb)	PP2A Cα (aa 153-309)	1/5000	BD Transduction Laboratories
pS262 (poly)	pS262-tau	1/200–500	Biosource
pS205 (poly)	pS205-tau	1/1000	Biosource
PHF-1 (mAb)	pS396/404-tau	1/500	Reference 14
AT8 (mAb)	pS199/S202/T205-tau	1/500–1000	Innogenetics
AT180 (mAb)	pT231/S235-tau	1/1000	Innogenetics
Tau-1 (mAb)	Non-pS198/199/202-tau	1/30,000	Reference 14
R134d (poly)	Total tau	1/1000	Reference 14
Tau-5 (mAb)	Total tau	1/1000	Biosource
Anti PTP-1B(poly)	PTP1B	1/1000	Upstate
Anti-actin (poly)	Actin	1/1000	Sigma

p, phosphorylated; Non-p, non-phosphorylated; Poly, rabbit polyclonal antibody; mAb, mouse monoclonal antibody.

Table 2 Detailed information for the cases used in immunohistochemistry

Case	Sex	Age	Brain weight (g)	Clinical diagnosis
1	F	85	1072	Control
2	F	64	1200	Control
3	M	71	1433	AD
4	F	91	1230	AD
5	F	83	1012	AD
6	M	92	1140	AD
7	F	65	700	AD
8	M	85	930	AD

Extract preparation and protein measurement

After treatment, cells were washed with ice-cold phosphate-buffered saline (PBS), then harvested, suspended in cell lysate buffer containing 2 mM ethylene glycol tetraacetic acid (EGTA), 50 mM NaF, 2 mM NaVO4, 0.5 mM phenylmethylsulfonyl fluoride, 5 mM ethylenediaminetetraacetic acid (EDTA), 150 mM NaCl, 50 mM Tris-HCl (pH 7.4), 1% Triton X-100, protease-inhibitor cocktail (1:200). After sonicating, samples were then kept on ice for 20 min. Homogenates from brains of transgenic APPswe /PS1 (A246E) and control mice, WT, ER$\alpha^{-/-}$ and ER$\beta^{-/-}$ mice, and AD and controls were prepared in buffer including 50 mM Tris, pH 7.0, 2.5 mM EDTA, 2.5 mM EGTA, 2 mM benzamidine, 1.0 mM phenylmethylsulfonyl fluoride, 0.1% β-mercaptoethanol, 20 mM β-glycerophosphate, 0.1% protease inhibitor cocktail, 2 μM sodium vanadate, 50 mM NaF and 2% sodium dodecyl sulfate (SDS) at 4°C.

Protein concentrations of all samples were detected with the bicinchoninic acid (BCA) assay kit (Sigma-Aldrich, Stockholm, Sweden), and then samples were stocked at -70°C until used.

PTP1B dephosphorylation of PP2A

10 μg homogenate of human brain tissue in homogenate buffer without protein phosphatase inhibitors were incubated with 0.05u, 0.2u and 0.4u purified PTP1B (Sigma-Aldrich, Stockholm, Sweden). One unit is considered to hydrolyse 1 μM phosphopeptide substrate epidermal growth factor receptor (EGFR) fragment 988–998 per minute at pH 7.2 at

30°C in 20 μl phosphatase reaction buffer (25 mM Hepes, pH 7.0, 2 mM EDTA, 0.1 mg/ml BSA, 30 mM β- mercaptoethanol) at 30°C for 1.5 hrs. The reactions were stopped by adding 20 μl of 2 X Laemmli sample buffer for SDS gel electrophoresis.

Dot and Western blots

For dot blots, boiled homogenates, supernatant and pellet fractions from 10 control and 21 AD cases (Table 3) were spotted on nitrocellulose membrane in triplicates (4 μg protein/dot). For Western blots, boiled samples were electrophoresed in 10% SDS-polyacrylamide gel and the separated proteins transferred to nitrocellulose membranes. The membrane was then dried and blocked in 5% non-fat milk for 1 hr at room temperature. Incubations with antibodies to PP2Ac-Yp307, total PP2A (R123d), tau antibodies and actin antibody were performed at 4°C overnight. Membranes from dot and Western blots that were incubated with primary antibodies were detected using horseradish peroxidase-linked anti-rabbit or antimouse IgGs (Amersham Biosciences AB, Uppsala, Sweden) at 1:2000 dilution, then visualized by the enhanced chemiluminescence kit (Amersham Biosciences AB). Intensities of positive bands or spots were quantified with Discovery Series Quantity One 1-D Analysis Software (Bio-Rad Laboratories, Inc., Stockholm, Sweden).

Immunohistochemistry, and double immunofluorescene confocal microscopy

For immunohistochemistry of the human brain tissues, formalin-fixed tissue blocks (Table 2) were soaked two days each in 15% and 30% sucrose, and were then then frozen and sectioned at 20 μm. Following the protocols previously described [28], sections were blocked with 5% bovine serum albumin (BSA) for 30 min., then incubated for 44–48 hrs at 4°C with rabbit polyclonal antibody to PP2Ac-Yp307 (1:100), followed by incubation with biotinylated anti-rabbit IgG (1:200) for 2 hrs and visualized with the avidin-biotin-peroxidase complex kit (Vector, Burlingame, CA, USA) with 3-3′-diaminobenzidine-4 HCl/H_2O_2 (DAB; Sigma, St. Louis, MO, USA) as substrate.

The formalin-fixed paraffin-embedded tissue blocks from rat brains were sectioned at 4 μm. After deparaffination and washing, heat-induced antigen retrieval was accomplished by immersing slides placed in Tissue-Tek slide holders in an autoclave for 5 min. and then cooled to room temperature. After washing with PBS three times, endogenous peroxidase activity was blocked with 3% H_2O_2 for 10 min. at room temperature. Sections were incubated with primary antibodies PHF-1 (1:200) and PP2Ac-Yp307 (1:50), respectively, overnight at 4°C. After washing with PBS, the sections were blocked with the reagent 1 (polymer helper), incubated with the reagent 2 (poly peroxidase-antimouse/rabbit IgG) and then visualized with DAB as substrate. Counterstaining with haematoxylin was also done. For double immunofluorescent stainings, sections from fixed human brain tissue were immunostained with rabbit polyclonal antibody to PP2Ac-Yp307 and mAb AT8 or mAb 4G8, then the bound antibodies were labelled with CY3-conjugated secondary anti-rabbit IgGs (red, PP2Ac-Yp307), and CY2-conjugated secondary antimouse IgGs (green, mAb AT8, or 4G8) (Jackson ImmunoResearch Laboratories, Inc., West Grove, PA, USA). A BioRad Laser Scanning Confocal Imaging System (Radiance Plus; Bio-Rod House, Hertfordshire, UK) was used to determine the co-localization of the CY3-labelled PP2Ac-Yp307 and the CY2-labelled AT8 or 4G8.

PTP1B RNA interference

Annealed double stranded RNA duplexes (5′CGAACAGAGUCUAAUCUCAtt3′) corresponding to mouse PTP1B (Ambion, Cambridgeshire, UK) were transfected with 50 nM lipofectamine 2000 (Invitrogen, Stockholm, Sweden) into cultured mouse N2a cells. The effects of RNAi on PTP1B expression, and on phosphorylation of PP2A (Y307) and tau were measured after effectively silencing the target PTP1B gene expression (72 hrs). A non-targeting SiRNA (Silencer Negative Control 1 SiRNA, Ambion, Cambridgeshire, UK) was used as SiRNA transfection negative control.

Protein phosphatase activity assay

PP2A activity in the supernatants was assayed using the phosphatase kit V2460 (Promega, Madison, WI, USA). Briefly, endogenous free phosphate was removed from supernatants, and then the extracts were normalized for protein content. 5 μg protein samples in triplicates were incubated with a chemically synthesized phosphopeptide (RRA(pT)VA), an optimal substrate for PP2A, PP2B and PP2C, but not for PP1 in the buffer optimized for PP2A activity while cation-dependent PP2B and PP2C were inhibited (protocol provided by the manufacturer) for 30 min. at 33°C. Phosphate released from the substrate was detected by measuring the absorbance of a molybdate-malachite green-phosphate complex at 630 nm. PP2A activity was evaluated by the release of phosphate per μg protein and per minute (pmol/μg/min).

Table 3 Detailed information for the cases used in dot blots

Case	Age	Sex	Clinical diagnosis	Post-mortem delay (hrs)	Braak's neurofibrillary staging
1	67	M	Control	2	I
2	76	M	Control	3	III
3	96	F	Control	10	IV
4	75	M	Control	10	I
5	79	M	Control	5	IV
6	84	F	Control	7	IV
7	84	M	Control	7	III
8	83	M	Control	8	III
9	98	F	Control	9	III
10	82	F	Control	4	IV
11	86	M	AD	7	III
12	71	M	AD	7	III
13	76	F	AD	6	VI
14	88	M	AD	7	V
15	73	F	AD	7	V
16	82	M	AD	6	V
17	100	F	AD	6	V
18	90	F	AD	10	IV
19	74	F	AD	6	VI
20	84	F	AD	7	VI
21	92	F	AD	6	VI
22	78	F	AD	6	V
23	97	F	AD	9	V
24	68	F	AD	4	VI
25	91	F	AD	4	V
26	84	F	AD	4	V
27	86	F	AD	3	VI
28	54	F	AD	3	VI
29	82	F	AD	7	VI
30	74	F	AD	4	VI
31	87	F	AD	5	VI

Average age (years): Control, 82.40±9.30; AD, 81.76±10.62 ($P > 0.05$ *versus* control). Average post-mortem delay (hrs): Control, 6.50±2.88; AD, 5.90±1.81 ($P > 0.05$ *versus* control).

Statistical analysis

Non-paired Student's t-tests were used to analyse the possible changes between treated and non-treated cells, and transgenic and non-transgenic mice. One-way ANOVAs were used to analyse the difference of data from the brains at different neurofibrillary stages according to Braak and Braak' criteria. The Pearson correlation and stepwise regression between levels of PP2Ac-Yp307 and tau phosphorylation were also analysed. The significance level was set at $P<0.05$.

Results

Characterization of the antibody to phosphorylated PP2A (Y307)

Since *in vitro* phosphorylation of PP2A at the Y307 site potently inactivates PP2A [11], the antibody to PP2A phosphorylated at the Y307 site should recognize the inactivated PP2A (inactive form). The specificity of the affinity-purified antibody to PP2Ac-Yp307 was characterized by Western blots in homogenates from AD and control brains (15 μg protein/lane), purified AD p-tau and PHF-tau (2 μg protein/lane), and NIH-3T3 cell extracts with or without treatment of serum (Fig. 1A). A single positive band that corresponds to the PP2A catalytic subunit at approximately 36 kD appeared in the homogenates and NIH-3T3 cell extracts, but not in AD p-tau or PHF-tau, indicating that this antibody specifically recognized PP2A and did not cross-react with tau protein. A dramatic increase of PP2Ac-Yp307 was seen in the NIH-3T3 cell extracts treated with serum.

To confirm whether this antibody specifically recognizes tyrosine phosphorylated PP2A, human brain homogenates were incubated with purified PTP1B *in vitro* to release the phosphate from tyrosine sites; and samples were subjected to Western blots immunostained with anti-pPP2A (Y307). After PTP1B treatment, the positive band at 36 kD almost disappeared (Fig. 1B).

To further confirm the specificity of the antibody to PP2Ac-Yp307, immunostainings of the antibody absorbed with or without the corresponding blocking peptide (the short amino acid sequence containing pY307 of PP2A) were performed on the sections from AD brains. The immunostaining was hardly seen in sections treated with the blocking peptide, as compared to the sections without the blocking peptide absorption (Fig. 1C).

Immunoreactivity of inactive form of PP2A (Y307) in the AD brain

AD brains showed numerous neurons positive for the inactive form of PP2Ac-Yp307. The positive structures were more intensive in the entorhinal cortex, the hippocampal CA1, and the temporal cortex of AD brains (Fig. 2A) as compared to controls (data not shown). A large number of immunopositive neurons showed tangle-like inclusions and granular structures in cytoplasma (Fig. 2A: a–f, b1, d1, f1). Double-immunofluorescent stainings were carried out with antibodies to inactive form of PP2A (Y307) and mAb AT8 (PHF-tau) or mAb 4G8 (human Aβ17-26) in the sections of AD brains (Fig. 2B). PHF-tau immunoreactivity labelled by AT8 was restricted to neurons affected by NFTs and pre-tangles. In addition, SPs labelled by 4G8 were surrounded by NFTs positive for an inactive form of PP2Ac-Yp307 (Fig. 2B). During experiments, the control sections without primary antibodies were routinely used, and they showed negative staining (data not shown).

According to the immunoreactivity against inactive form of PP2Ac-Yp307 and mAb AT8, four different staining patterns of neurons could be distinguished under confocal microscopy in the hippocampal CA1 area of AD brains. Pattern 1 neurons were AT8-negative but showed granular staining for PP2Ac-Yp307 in the cytoplasm (Fig. 3, A1, A2 and A3). Pattern 2 neurons showed aggregates positive for both AT8 labelled-PHF-tau and PP2Ac-Yp307 as granules in the soma and neuropil threads, while the nuclear shape and position were relatively normal-looking (Fig.3, B1, B2 and B3). Pattern 3 neurons were classic NFTs, which showed some filamentous structures in the neuronal soma that stained positively for both PP2Ac-Yp307 and PHF-tau labelled by AT8. The cell nucleus of this kind of neuron was round but the nuclear position was distorted (Fig. 3, C1, C2 and C3). Pattern 4 neurons showed advanced tangles labelled by AT8 and the filamentous structures completely overlapped with PP2Ac-Yp307 (Fig. 3, D1, D2 and D3). The cell nucleus of this kind of neuron disappeared.

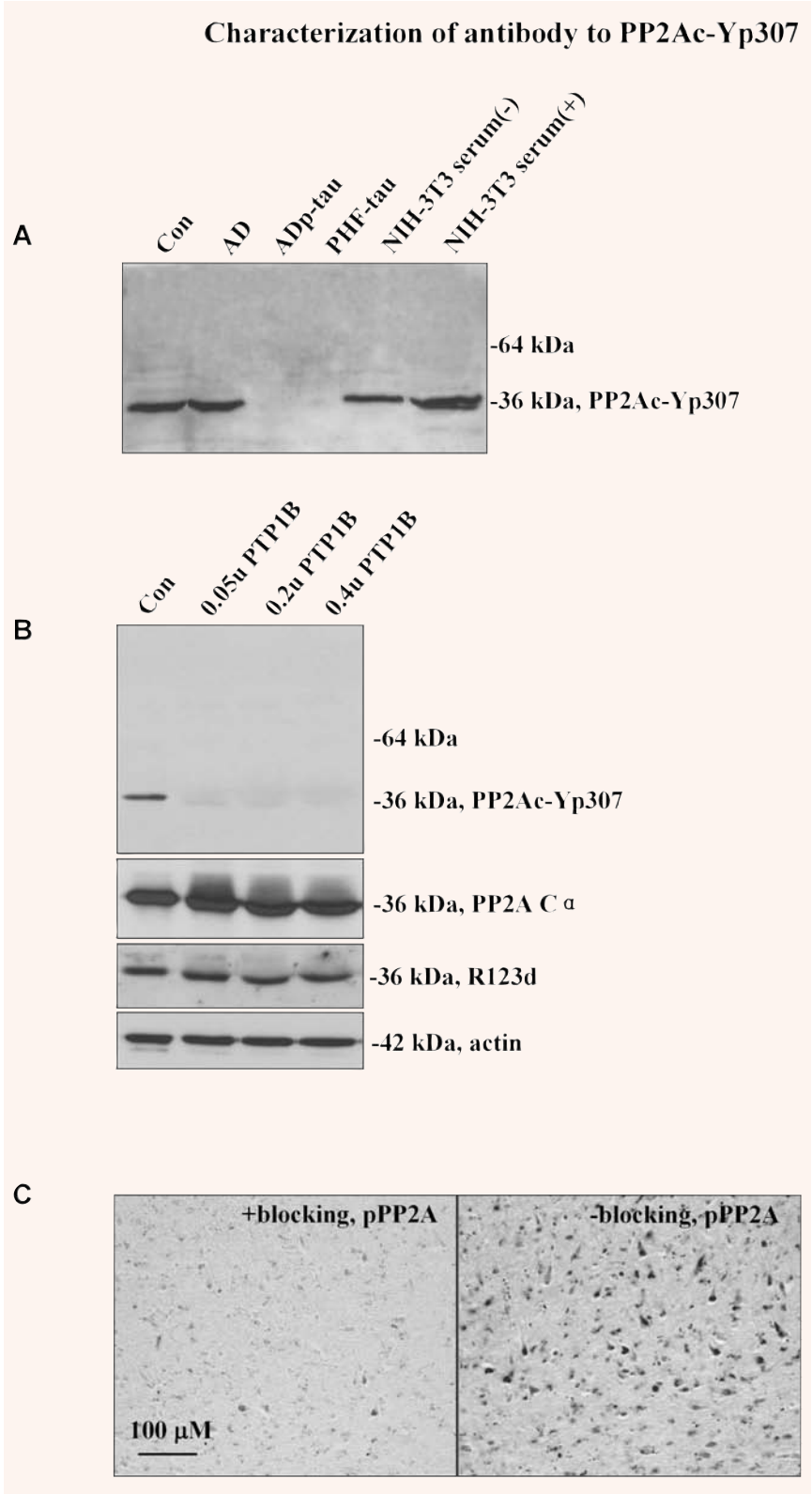

Fig. 1 Characterization of the antibody to protein phosphatase 2A (PP2A) catalytic subunit phosphorylated (p) phosphorylated at Y307. Samples from control (Con) and Alzheimer's disease (AD) brain homogenates (15 μg /lane), AD p-tau (2 μg /lane), paired helical filaments (PHF)-tau (2 μg/lane), and extracts from non-treated (-) and serum-treated (+) NIH-3T3 cell lysates (control cell extracts, Cell signalling) were separated by 10% SDS-PAGE, and the membranes were developed with antibody to PP2Ac-Yp307 (**A**). Positive staining appeared at 36 kD that corresponds to the molecular mass of the catalytic subunit of PP2A molecular mass in homogenates and NIH-3T3 cell lysates, but not in AD p-tau or PHF-tau. In (**B**), human brain tissue homogenates were incubated with purified PTP1B to remove the phosphate on tyrosine sites. After the reaction the homogenates were separated by 10% SDS-PAGE, and the membranes were developed with antibody to PP2Ac-Yp307. No signal was detected by anti-pPP2A (Y307) after PTP1B treatment. In (**C**), representative pictures from sections of AD brains were immunostained with the antibody to PP2Ac-Yp307 in the presence of the corresponding blocking peptide or not. The sections absorbed with the blocking peptide (+) hardly showed any positive neuronal staining, as compared to sections without blocking peptide absorption (-). Data from Western blots and immunohistochemistry indicated that the antibody to PP2Ac-Yp307 is specific.

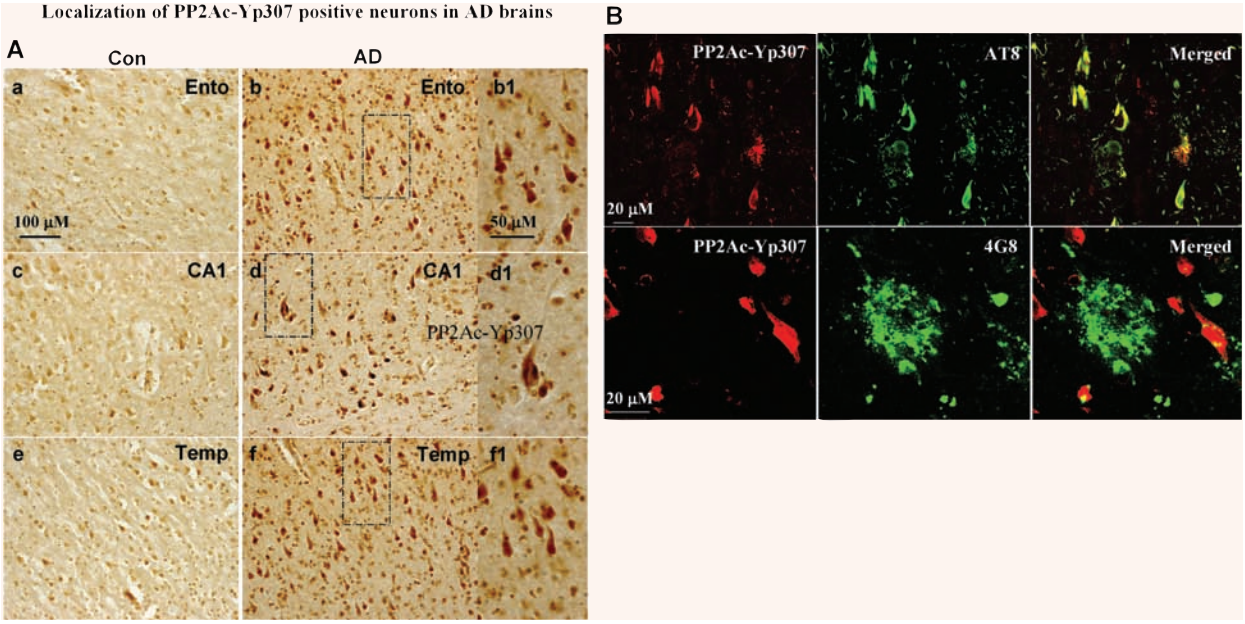

Fig. 2 Distribution of inactivated PP2Ac-Yp307 in AD and control (Con) brains. A larger number of intensively stained neurons positive for PP2Ac-Yp307 was found in the entorhinal (Ento) cortex, the hippocampus CA1 and the temporal cortex (Temp) of AD as compared to controls (**A**). Immunoreactivities of inactive form of PP2A were co-localized with PHF-tau labelled by AT8 that closely surrounded the senile plaques labelled by 4G8 (**B**).

The number of different patterns of neurons positive for PP2Ac-Yp307was counted in 28 continuous fields in relation to AT8 immunoreactivity in area CA1 of the hippocampus from three brains at Braak's neurofibrillary stages V-VI (same magnification as in Fig. 2B). Pattern 1 neurons were selectively positive for PP2Ac-Yp307 [number of neurons positive for PP2Ac-Yp307/AT8: 67/0]. In pattern 2 neurons, all neurons positive for PP2Ac-Yp307 co-existed with AT8 immunoreactivity, but some AT8-positive neurons were not labelled by the antibody to PP2Ac-Yp307 [number of neurons positive for PP2Ac-Yp307/AT8: 27/33]. All of the AT8-positive pattern 3 and 4 neurons co-existed with neurons positive for PP2Ac-Yp307 [number of neurons positive for PP2Ac-Yp307/AT8: 101/101]. The four distinguishable patterns of neurons suggest that a progressive development of Alzheimer's tau pathologies from pre-tangle neurons to NFT-bearing neurons might involve phosphorylation of PP2A at the Y307 site.

Levels of phosphorylated PP2A (Y307) in AD and control brains

In order to investigate the degree of PP2A inactivation seen by immunohistochemistry in AD brains, levels of total PP2A (by R123d and anti-PP2A C?) and PP2Ac-Yp307 were measured in homogenates, supernatants, and pellets (100,000 g) of 10 control and 21 AD cases by dot blots. As shown in Fig. 4A and B, there were no significant differences in total PP2A levels in homogenates and supernatants (100,000 g) between AD and control groups. However, total PP2A levels were significantly lower in the pellets of AD brains than in control brains, as detected by both R123d ($P<0.05$) and anti-PP2A Cα ($P<0.01$), indicating dramatically decreased levels of total PP2A in insoluble fractions containing aggregated proteins such as PHF-tau. In contrast to total PP2A, levels of PP2Ac-Yp307 in the pellets did not differ between AD and control brains (Fig. 4C). After

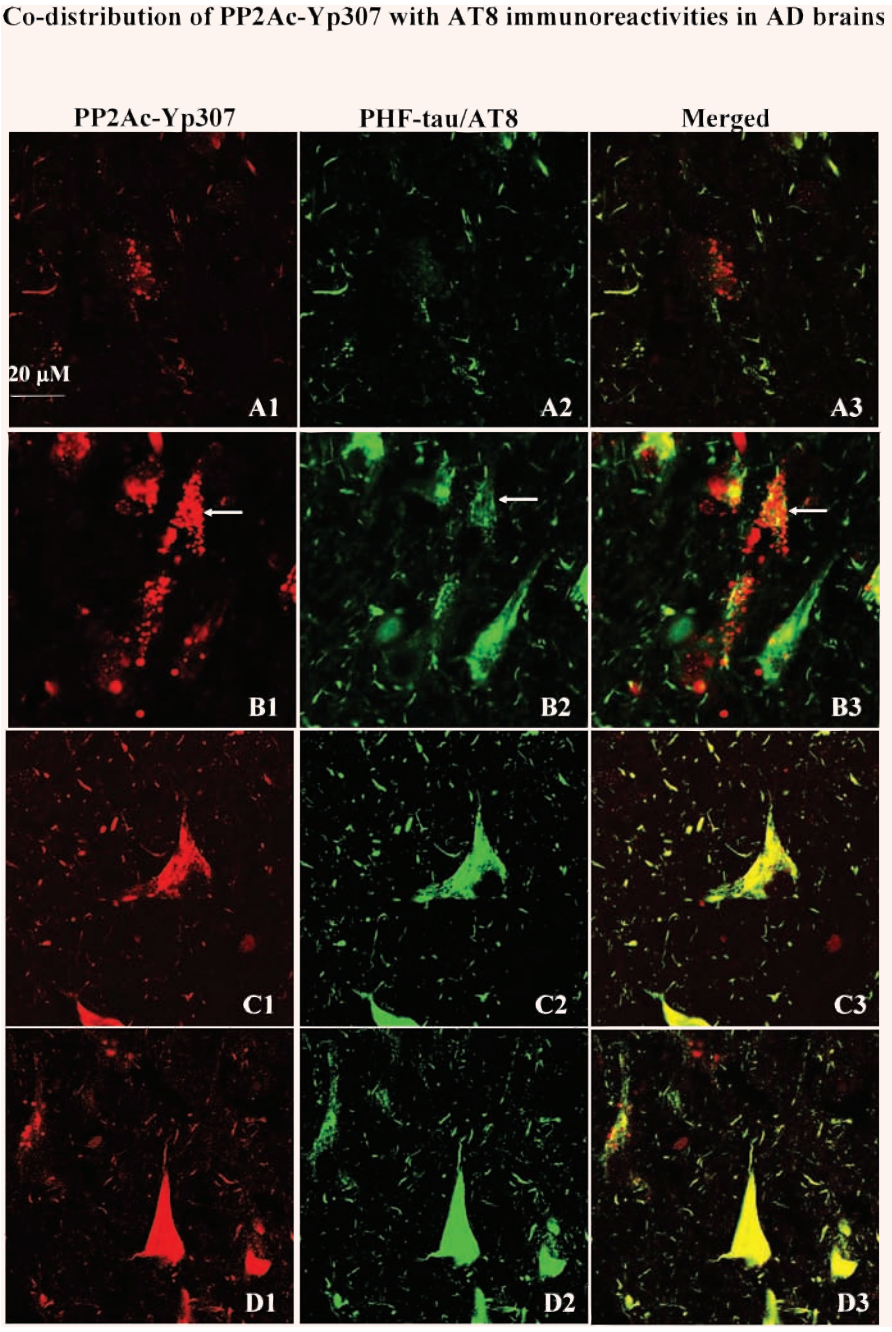

Fig. 3 Immunoreactivities of inactivated PP2Ac-Yp307 in neurons with different extents of paired helical filaments (PHF)-tau accumulation labelled by AT8. In the normal-looking neurons, only antibody to PP2Ac-Yp307 was positive in granular structures (**A1**, **A2** and **A3**). The pre-tangle neurons contained inclusions of granular structures that are positive for antibody to PP2Ac-Yp307 and AT8, but the nuclear shape still looked normal (**B1**, **B2** and **B3**, white arrow indicated). The classic neurofibrillary tangles (NFT)-bearing neurons showed granular aggregates positive for PP2Ac-Yp307 that distributed along the AT8-positive filamentous structures. The nucleus was positioned to the periphery of neuronal soma, but the nuclear shape was still relatively normal (**C1**, **C2** and **C3**). The advanced stage of NFT-bearing neurons showed fully overlapping filamentous immunoreactivities of the antibodies to PP2Ac-Yp307 and AT8. The nucleus was invisible (**D1**, **D2** and **D3**).

normalizing the inactivated pPP2A (Y307) with the total PP2A, sharply increased levels of PP2Ac-Yp307 were observed in the pellets of the AD group as compared with controls (data not shown).

In comparison with Braak's stages I–II (Fig. 4D), a significant increase of PP2Ac-Yp307 levels was observed at stages III–IV ($P<0.05$), although the levels of total PP2A did not change. The levels of PP2Ac-Yp307 normalized to the levels of total PP2A (both R123d and anti-PP2A Cα) showed a positive linear relationship between Braak's neurofibrillary stages and the level of PP2Ac-Yp307 (Fig. 4E).

As shown in Table 4, levels of PP2Ac-Yp307 showed significant correlation with tau phosphoryla-

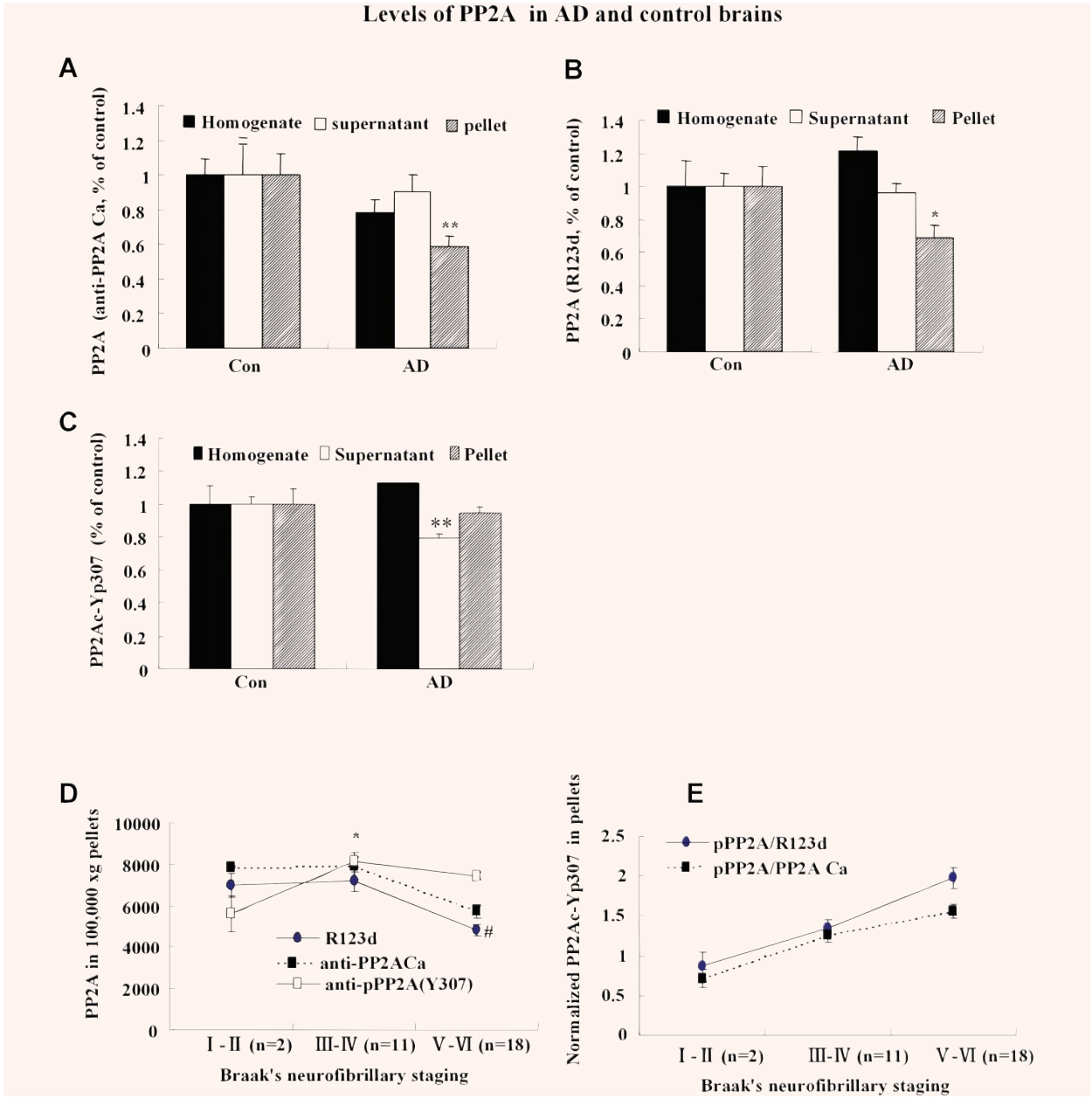

Fig. 4 Levels of inactivated PP2Ac-Yp307 in AD and control brains. Levels of total PP2A (by R123d and Anti-PP2A Cα) and PP2Ac-Yp307 were measured in the homogenates, supernatants and pellets (100,000× g) of 21 AD and 10 control cases by dot blots. (**A**) showed only a significant decrease of total PP2A by Anti-PP2A Cα in 100, 000× g pellet fraction of AD as compared to the control (**, $P < 0.01$). (**B**) showed only a significant decrease of total PP2A by R123d in 100, 000× g pellet fraction of AD as compared with the control (*, $P < 0.05$). (**C**) showed only a significant decrease of PP2Ac-Yp307 in 100,000× g supernatants in AD as compared with the control (**, $P < 0.01$). (**D**) showed significant changes of PP2Ac-Yp307 and total PP2A in 100,000× g pellets of cases at different Braak's neurofibrillary stages (*$P < 0.05$, between stages III–IV and stages I–II; #$P < 0.05$ by R123d between stages III–IV and stages V–VI). (**E**) showed a linear increase of the ratio of PP2Ac-Yp307 / total PP2A in 100,000× *g* pellets of cases at different Braak's neurofibrillary stages. All the results were represented by the mean ± SEM.

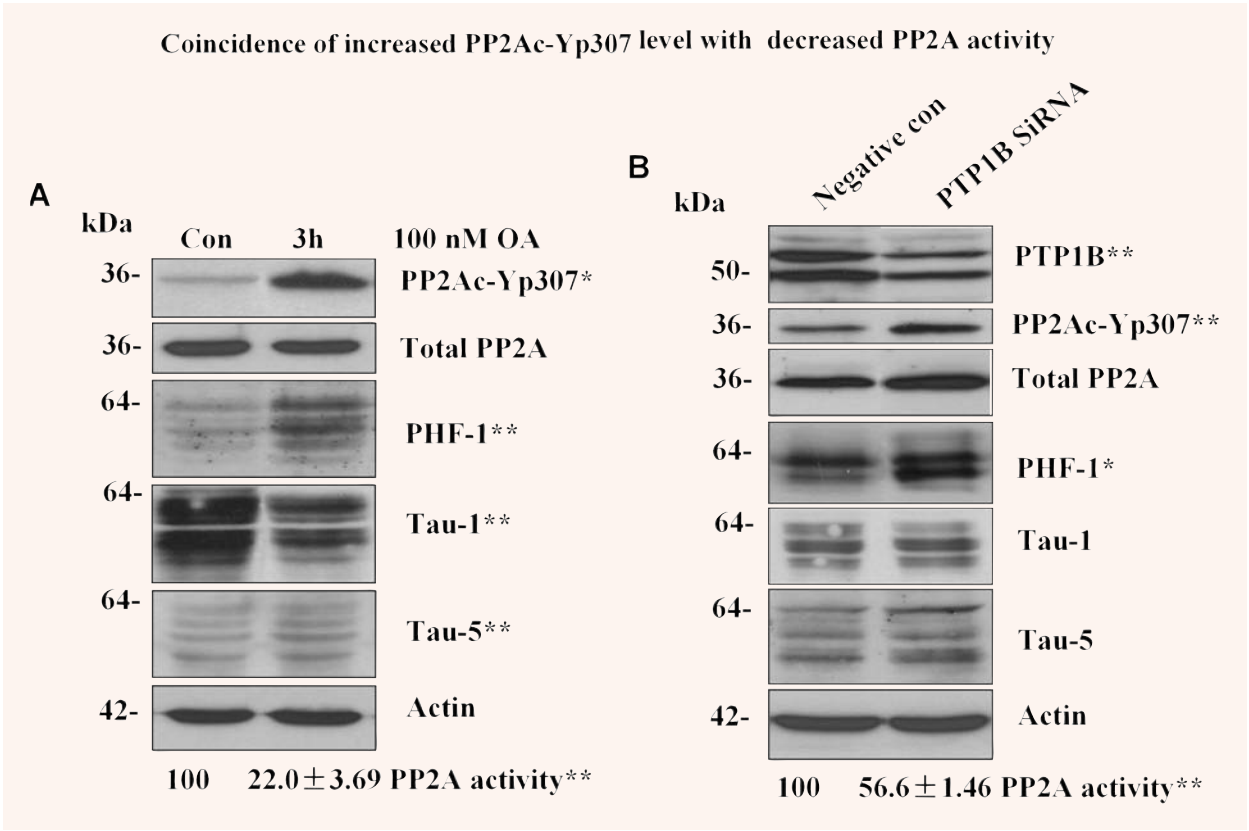

Fig. 5 Inactivated PP2Ac-Yp307 in wild-type N2a cells treated with okadaic acid (OA) or PTP1B SiRNA. After N2a cells were treated with 100 nM OA for 3 hrs, a significant increase of PP2Ac-Yp307 was observed, which coincides with the significant decrease of PP2A activity, and the significant increase of tau phosphorylation at PHF-1 and significant decrease of tau dephosphorylation at Tau-1 sites (**A**). N2a cells transfected with specific interfering RNA to PTP1B showed a significant decrease of PTP1B expression, which is in parallel to the significant increase of PP2Ac-Yp307, the significant decrease of PP2A activity, and the significant increase of tau phosphorylation at PHF-1 sites. All the results (mean ± SEM) were from at least three independent experiments. * P<0.05; ** P<0.01.

Table 4 Correlations of inactivated PP2Ac-Yp307 with tau in 100, 000× g pellets

Antibodies to tau	to PP2Ac-Yp307	
	r	P
AT8 (p-tau)	0.359	0.047 *
PHF-1 (p-tau)	0.357	0.048 *
Tau-1 (de-ptau)	–0.606	0.000 **
R134d (total tau)	0.225	0.223

p-tau, phosphorylated tau; de-ptau, unphosphorylated tau; r, Pearson correlation coefficient. * P < 0.05; ** P < 0.01.

tion at AT8 sites (P = 0.047) and PHF-1 sites (P = 0.048), and tau dephosphorylation at Tau-1 sites (P = 0.000), but not with total tau (R134d, P = 0.223) in the pellets (100,000 g) of AD and control cases.

Effects of okadaic acid or partial knockout of PTP1B on PP2A phosphorylation (Y307) in wild-type N2a cells

Since phosphorylation of PP2A (Y307) induced by okadaic acid (OA) affects PP2A activity *in vitro* [11], interaction of PP2Ac-Yp307 and OA treatment in

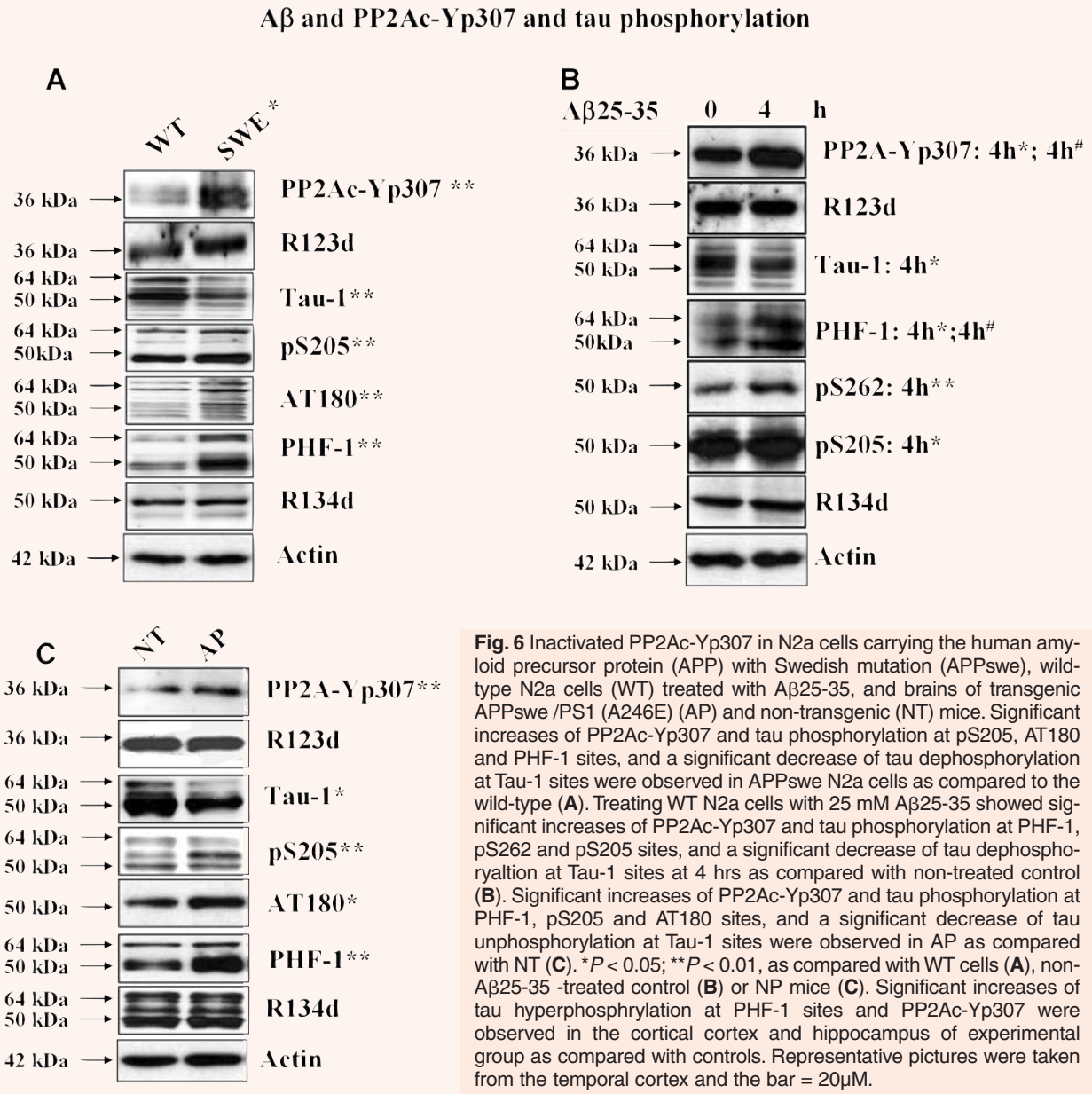

Fig. 6 Inactivated PP2Ac-Yp307 in N2a cells carrying the human amyloid precursor protein (APP) with Swedish mutation (APPswe), wild-type N2a cells (WT) treated with Aβ25-35, and brains of transgenic APPswe /PS1 (A246E) (AP) and non-transgenic (NT) mice. Significant increases of PP2Ac-Yp307 and tau phosphorylation at pS205, AT180 and PHF-1 sites, and a significant decrease of tau dephosphorylation at Tau-1 sites were observed in APPswe N2a cells as compared to the wild-type (**A**). Treating WT N2a cells with 25 mM Aβ25-35 showed significant increases of PP2Ac-Yp307 and tau phosphorylation at PHF-1, pS262 and pS205 sites, and a significant decrease of tau dephosphoryaltion at Tau-1 sites at 4 hrs as compared with non-treated control (**B**). Significant increases of PP2Ac-Yp307 and tau phosphorylation at PHF-1, pS205 and AT180 sites, and a significant decrease of tau unphosphorylation at Tau-1 sites were observed in AP as compared with NT (**C**). $^{*}P < 0.05$; $^{**}P < 0.01$, as compared with WT cells (**A**), non-Aβ25-35 -treated control (**B**) or NP mice (**C**). Significant increases of tau hyperphosphrylation at PHF-1 sites and PP2Ac-Yp307 were observed in the cortical cortex and hippocampus of experimental group as compared with controls. Representative pictures were taken from the temporal cortex and the bar = 20μM.

intact cells was investigated in the current study. In cultured N2a cells, OA at 100 nM (a potent PP2A inhibitor) induced a significant reduction of PP2A activity (~80%, $P<0.05$) (Fig. 5A), which corresponds to the dramatic increases of PP2Ac-Yp307 and phosphorylation of tau at PHF-1 sites, and to the dramatic decrease of tau dephosphorylation at Tau-1 sites ($P<0.01$; Fig. 5A). Total PP2A level showed no significant increase (Fig. 5A). PTP1B was previously shown to affect PP2A phosphorylation at the Y307 site *in vitro* [11]. As shown in Fig. 5B, the significantly increased PP2Ac-Yp307 levels were observed

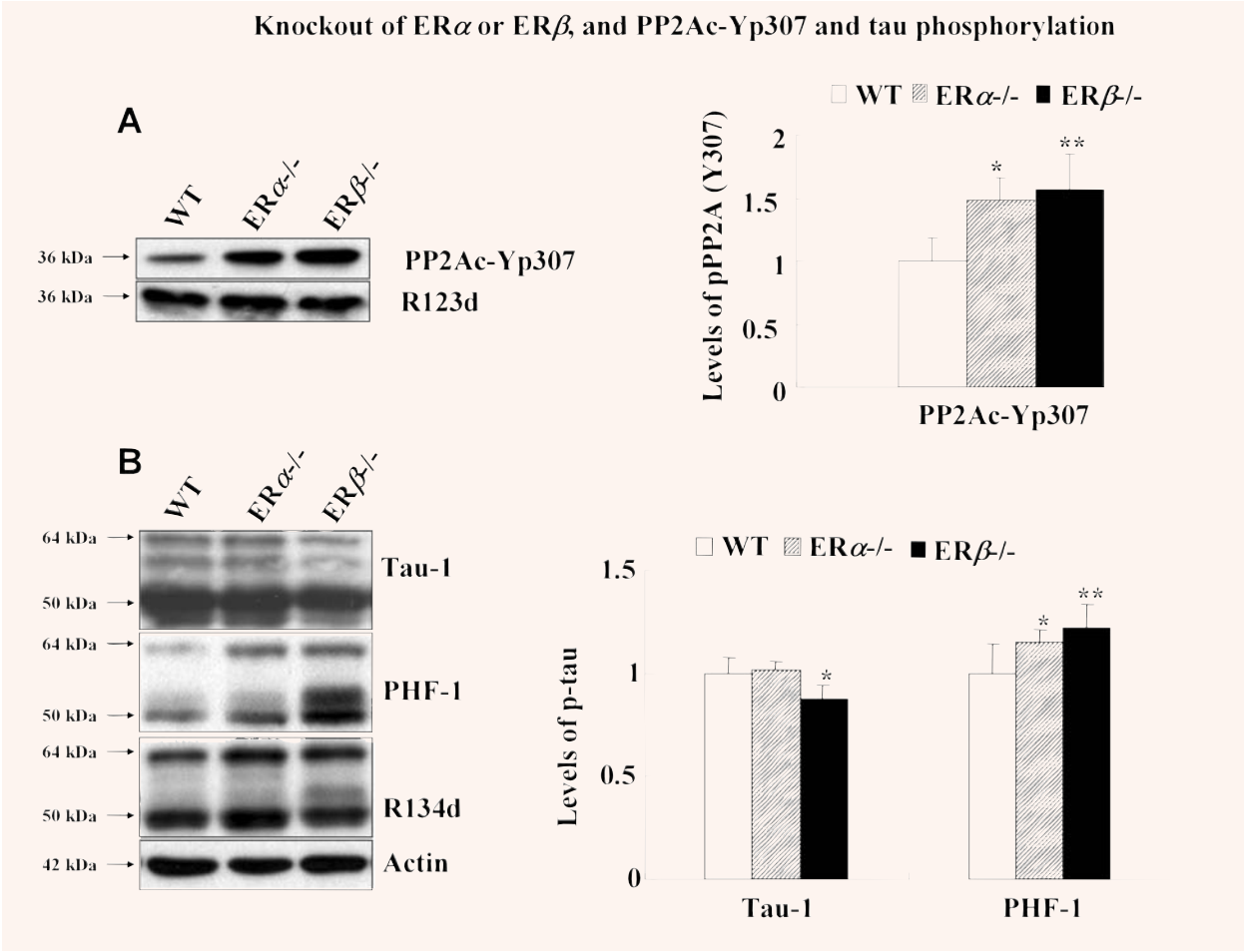

Fig. 7 Phosphorylated (p) /inactivated PP2Ac-Yp307 in brains of oestrogen receptor (ER)$\alpha^{-/-}$ and ER$\beta^{-/-}$ mice. By Western blots (7 μg /lane), levels of PP2Ac-Yp307 and p-tau at PHF-1 sites were significantly increased in ER$\alpha^{-/-}$ or ER$\beta^{-/-}$ as compared to wild-type (WT) mice. The level of de-ptau at Tau-1 sites was significantly decreased only in ER$\beta^{-/-}$ as compared with the WT control. Data were presented by mean ± SD from five mice each group (n = 5). *P<0.05 and **P<0.01 between ER$\alpha^{-/-}$ or ER$\beta^{-/-}$ and control mice.

after PTP1B silencing, in parallel to a significant decrease in PP2A activity (~50%) and tau phosphorylation at PHF-1 sites.

Effect of Aβ on PP2A phosphorylation (Y307)

As compared with WT N2a cells, a significant increase of PP2Ac-Yp307 was observed in APPswe N2a cells (P<0.01). This was accompanied by in parallel significant increases in tau phosphorylation at the S205 (pS205), T231/S235 (AT180), and PHF-1 sites, and a significant decrease of tau dephosphorylation at Tau-1 sites (Fig. 6A).

In WT N2a cells treated with Aβ25-35, a similar pattern of changes were observed for PP2Ac-Yp307 and tau at PHF-1, Tau-1 and pS205 sites (Fig. 6B). In general, the Aβ-induced increase of PP2Ac-Yp307 and tau phosphorylation was most pronounced after 4 hrs of treatment.

In the brains of 16-month-old transgenic APPswe /PS1 (A246E) mice with numerous β-amyloid plaques [32], the levels of PP2Ac-Yp307 were significantly increased (P<0.01), in parallel with a signifi-

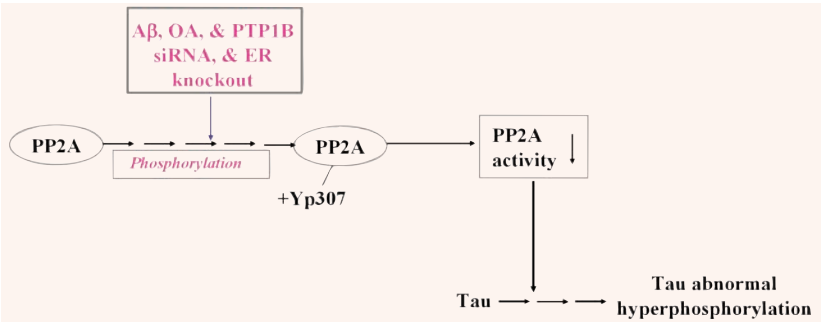

Fig. 8 Hypothetical scheme showing that PP2A phosphorylation (Y307) can be induced by Aβ, okadaic acid, PTP1B knockout or knockout of oestrogen receptor (ER) a and ERβ, which can inactivate PP2A. PP2A inactivation results directly in the increase of tau phosphorylation.

cant increase of tau phosphorylation at pS205, AT180 and PHF-1 sites, and a significant decrease of tau dephosphorylation at Tau-1 sites (Fig. 6C).

Knockout of ERα or ERβ *in vivo* leads to increased PP2A (Y307) phosphorylation

In order to see the effects of oestrogen deficiency, we investigated the levels of PP2Ac-Yp307 and tau phosphorylation in brain homogenates of WT, $ER\alpha^{-/-}$, and $ER\beta^{-/-}$ mice by Western blots. A significant increase of PP2Ac-Yp307 was observed in both $ER\alpha^{-/-}$ ($P<0.05$) and $ER\beta^{-/-}$ ($P<0.01$) mice (Fig. 7A). The levels of dephosphorylated tau at Tau-1 sites were significantly decreased only in $ER\beta^{-/-}$ mice, while the levels of tau phosphorylated at PHF-1 sites were significantly increased in both $ER\alpha^{-/-}$ ($P<0.05$) and $ER\beta^{-/-}$ brains ($P<0.01$) (Fig. 7B).

Discussion

Investigating the mechanism of reduced PP2A activity in AD brain is critical to our understanding of the pathogenesis of AD-related tau pathology. According to the amyloid cascade hypothesis, Aβ is thought to be the upstream cause of NFT formation but the underlying mechanism has not been identified [16]. A number of studies have suggested that Aβ accumulation or oestrogen deficiency can activate protein kinases, which can phosphorylate tau at sites seen in AD brains [19–24]. The current study proposes that Aβ accumulation or the oestrogen deficiency may mediate the up-regulation of PP2A phosphorylation (Y307), which in turn contributes to the reduced PP2A activity in the AD brain (Fig. 8).

Decreased levels of PP2A ABaC enzyme and PP2A mRNA, down-regulated carboxyl methylation of PP2A catalytic subunit and up-regulated PP2A inhibitors have been reported in AD brains [1, 5, 6, 10]. These factors and the post-translational modifications of PP2A, such as PP2A demethylation at the L309 site and PP2A phosphorylation at the Y307 site, may modulate PP2A activity [11, 12, 35, 36]. The current study is the first to characterize an antibody specifically recognizing the inactivated phosphorylated form of PP2Ac-Yp307, and to report that the PP2Ac-Yp307 is increased in the 100,000 g pellet fraction that contains NFTs, and that the PP2Ac-Yp307 is aberrantly accumulated in neurons that contain pre-tangles or NFTs in the AD brain. The pathological accumulation of PP2Ac-Yp307 in pre-tangle neurons precedes PHF-tau accumulation, suggesting that the post-translational modification of PP2A at the Y307 site might be an early event in the pathogenesis of AD-related tau pathology.

These findings on PP2A in the AD brain made us further investigate factors underlying the post-translational change in PP2A. Earlier studies have reported that Aβ can induce tyrosine phosphorylation of numerous proteins and activate tau kinases [18, 20–22]. Data from the current study showed that 4G8-positive SPs co-existed with tangle-bearing neurons positive for PP2Ac-Yp307 in close vicinity in the AD brain. This finding points to a link between Aβ accumulation and the post-translational modification of PP2A at the Y307 site. In order to explore the link, we conducted experiments employing three different experimental models (APPswe N2a cells, N2a cells treated with Aβ25-35 and brains of transgenic APPswe/PS1 (A246E) mice) and found that the up-regulated PP2A phosphorylation (Y307) correlates with tau phosphorylation at multiple sites.

In a similar manner to Aβ, up-regulated PP2A phosphorylation (Y307) was found in the brains of $ER\beta^{-/-}$ mice, which corresponds to increased tau phosphorylation at PHF-1 sites and decreased tau dephosphorylation at Tau-1 sites. Knockout of ERα induced a significant up-regulation of PP2A phosphorylation (Y307), which was accompanied by a significant increase of tau phopsphorylation at PHF-1 sites. Oestrogen has been reported to activate tau kinases such as PKB/Akt and GSK-3β [23, 24]. On the other hand, according to the present findings in ER knockout mice, oestrogen deficiency may mediate PP2A inactivation through post-translational modifications such as phosphorylation at the Y307 site, which likely overrides the inhibition of tau kinases induced by oestrogen deficiency. A recent large study found no effect of ovariectomy or oestrogen replacement therapy on the extent of amyloid pathology in APPswe/PS1(A246E) mice, but did not address tau phosphorylation [30]. Future studies should assess whether transgenic expression of mutated APP in ER knockout mice produces more SP and NFT pathology than in ER wild type mice. The candidate tyrosine kinase that commits the increased phosphorylation of PP2A at the Y307 site in AD brain will also be identified.

In conclusion, the regulation of PP2A activity towards tau dephosphorylation is a very complicated process, the data from the current study suggested that even phosphorylation of PP2A at the Y307 site is modulated by multiple factors co-existing in the AD brain, such as Aβ deposition and oestrogen deficiency.

Acknowledgements

Drs. Irina Alafuzoff and Hilkka Soininen (University of Kuopio, Finland) are thanked for providing human materials. mAb PHF-1 was given by Dr Peter Davies, Albert Einstein College of Medicine (Bronx, NY, USA), and mAb Tau-1 from Dr. L. Binder, Northwestern University (Chicago, IL, USA). Rabbit antiserum R134d to the longest isoform of recombinant human tau was a gift from Dr. K. Iqbal, New York State Institute for Basic Research in Developmental Disabilities (Staten Island, NY, USA). Dr. Sam Sisodia at the Department of Neurobiology, the University of Chicago is thanked for providing us with the APPswe N2a cells and Dr. David Borchelt at the University of South Florida (Gainsville, FL, USA) for providing founders for the APPswe/-PS1(A246E) mice.

References

1. **Tanimukai H, Grundke-Iqbal I, Iqbal K.** Up-regulation of inhibitors of protein phosphatase-2A in Alzheimer's disease. *Am J Pathol.* 2005; 166: 1761–71.
2. **Chung H, Nairn AC, Murata K, Brautigan DL.** Mutation of Tyr307 and Leu309 in the protein phosphatase 2A catalytic subunit favors association with the alpha 4 subunit which promotes dephosphorylation of elongation factor-2. *Biochemistry.* 1999; 38: 10371–6.
3. **Janssens V, Goris J.** Protein phosphatase 2A: a highly regulated family of serine/threonine phosphatases implicated in cell growth and signalling. *Biochem J.* 2001; 53: 417–39.
4. **Gong CX, Singh TJ, Grundke-Iqbal I, Iqbal K.** Phosphoprotein phosphatase activities in Alzheimer disease brain. *J Neurochem.* 1993; 61: 921–7.
5. **Vogelsberg-Ragaglia V, Schuck T, Trojanowski JQ, Lee VM.** PP2A mRNA expression is quantitatively decreased in Alzheimer's disease hippocampus. *Exp Neurol.* 2001; 168: 402–12.
6. **Sontag E, Luangpirom A, Hladik C, Mudrak I, Ogris E, Speciale S, White CL 3rd.** Altered expression levels of the protein phosphatase 2A ABalphaC enzyme are associated with Alzheimer disease pathology. *J Neuropathol Exp Neurol.* 2004; 63: 287–301.
7. **Pei JJ, Gong CX, An WL, Winblad B, Cowburn RF, Grundke-Iqbal I, Iqbal K.** Okadaic-acid-induced inhibition of protein phosphatase 2A produces activation of mitogen-activated protein kinases ERK1/2, MEK1/2, and p70 S6, similar to that in Alzheimer's disease. *Am J Pathol.* 2003; 163: 845–58.
8. **Liu R, Pei JJ, Wang XC, Zhou XW, Tian Q, Winblad B, Wang JZ.** Acute anoxia induces tau dephosphorylation in rat brain slices and its possible underlying mechanisms. *J Neurochem.* 2005; 94: 1225–34.
9. **Kins S, Crameri A, Evans DR, Hemmings BA, Nitsch RM, Gotz J.** Reduced protein phosphatase 2A activity induces hyperphosphorylation and altered compartmentalization of tau in transgenic mice. *J Biol Chem.* 2001; 276: 38193–200.
10. **Sontag E, Hladik C, Montgomery L, Luangpirom A, Mudrak I, Ogris E, White CL 3rd.** Downregulation of protein phosphatase 2A carboxyl methylation and methyltransferase may contribute to Alzheimer disease pathogenesis. *J Neuropathol Exp Neurol.* 2004; 63: 1080–91.

11. **Chen J, Martin BL, Brautigan DL.** Regulation of protein serine-threonine phosphatase type-2A by tyrosine phosphorylation. *Science.* 1992: 257: 1261–4.
12. **Chen J, Parsons S, Brautigan DL.** Tyrosine phosphorylation of protein phosphatase 2A in response to growth stimulation and v-src transformation of fibroblasts. *J Biol Chem.* 1994; 269: 7957–62.
13. **Brautigan DL.** Flicking the switches: phosphorylation of serine/threonine protein phosphatases. *Semin Cancer Biol.* 1995; 6: 211–7.
14. **Zhou XW, Li X, Bjorkdahl C, Sjogren MJ, Alafuzoff I, Soininen H, Grundke-Iqbal I, Iqbal K, Winblad B, Pei JJ.** Assessments of the accumulation severities of amyloid β-protein and hyperphosphorylated tau in the medial temporal cortex of control and Alzheimer's brains. *Neurobiol Dis.* 2006; 22: 657–68.
15. **Lewis J, Dickson DW, Lin WL, Chisholm L, Corral A, Jones G, Yen SH, Sahara N, Skipper L, Yager D, Eckman C, Hardy J, Hutton M, McGowan E.** Enhanced neurofibrillary degeneration in transgenic mice expressing mutant tau and APP. *Science.* 2001; 293: 1487–91.
16. **Gotz J, Chen F, van Dorpe J, Nitsch RM.** Formation of neurofibrillary tangles in P301l tau transgenic mice induced by Abeta 42 fibrils. *Science.* 2001; 293: 1491–5.
17. **Oddo S, Billings L, Kesslak JP, Cribbs DH, LaFerla FM.** Abeta immunotherapy leads to clearance of early, but not late, hyperphosphorylated tau aggregates via the proteasome. *Neuron.* 2004; 43: 321–32.
18. **Takashima A, Noguchi K, Sato K, Hoshino T, Imahori K.** Tau protein kinase I is essential for amyloid beta-protein-induced neurotoxicity. *Proc Natl Acad Sci USA.* 1993; 90: 7789–93.
19. **Singh M, Setalo G Jr, Guan X, Frail DE, Toran-Allerand CD.** Estrogen-induced activation of the mitogen-activated protein kinase cascade in the cerebral cortex of estrogen receptor-alpha knock-out mice. *J Neurosci.* 2000; 20: 1694–700.
20. **Stein TD, Johnson JA.** Lack of neurodegeneration in transgenic mice overexpressing mutant amyloid precursor protein is associated with increased levels of transthyretin and the activation of cell survival pathways. *J Neurosci* .2002; 22: 7380–8.
21. **Ghribi O, Prammonjago P, Herman MM, Spaulding NK, Savory J:** Abeta (1-42)-induced JNK and ERK activation in rabbit hippocampus is differentially regulated by lithium but is not involved in the phosphorylation of tau. *Brain Res Mol Brain Res.* 2003;119: 201–6.
22. **Wang Q, Walsh DM, Rowan MJ, Selkoe DJ, Anwyl R.** Block of long-term potentiation by naturally secreted and synthetic amyloid beta-peptide in hippocampal slices is mediated via activation of the kinases c-Jun N-terminal kinase, cyclin-dependent kinase 5, and p38 mitogen-activated protein kinase as well as metabotropic glutamate receptor type 5. *J Neurosci.* 2004; 24: 3370–8.
23. **Yu X, Rajala RV, McGinnis JF, Li F, Anderson RE, Yan X, Li S, Elias RV, Knapp RR, Zhou X, Cao W.** Involvement of insulin/PI3K/Akt signal pathway in 17beta-estradiol-mediated neuroprotection. *J Biol Chem.* 2004; 279: 13086–94.
24. **Mannella P, Brinton RD.** Estrogen receptor protein interaction with phosphatidylinositol 3-kinase leads to activation of phosphorylated Akt and extracellular signal-regulated kinase 1/2 in the same population of cortical neurons: a unified mechanism of estrogen action. *J Neurosci.* 2006, 26: 9439–47.
25. **Pei JJ, Khatoon S, An WL, Nordlinder M, Tanaka T, Braak H, Tsujio I, Takeda M, Alafuzoff I, Winblad B, Cowburn RF, Grundke-Iqbal I, Iqbal K:** Role of protein kinase B in Alzheimer's neurofibrillary pathology. *Acta Neuropathol.* 2003; 105: 381–92 .
26. **Kins S, Kurosinski P, Nitsch RM, Gotz J.** Activation of the ERK and JNK signaling pathways caused by neuron-specific inhibition of PP2A in transgenic mice. *Am J Pathol.* 2003; 163: 833–43.
27. **Kyoung Pyo H, Lovati E, Pasinetti GM, Ksiezak-Reding H.** Phosphorylation of tau at THR212 and SER214 in human neuronal and glial cultures: the role of AKT. *Neuroscience.* 2004; 127: 649–58 .
28. **An WL, Cowburnm RF, Li L, Braak, H., Alafuzoff, I, Iqbal K., Iqbal IG., Winblad B, Pei JJ.** Up-regulation of phosphorylated/activated p70 S6 kinase and its relationship to neurofibrillary pathology in Alzheimer's disease. *Am J Pathol.* 2003; 163: 591–607.
29. **Borchelt DR, Thinakaran G, Eckman CB, Lee MK, Davenport F, Ratovitsky T, Prada CM, Kim G, Seekins S, Yager D, Slunt HH, Wang R, Seeger M, Levey AI, Gandy SE, Copeland NG, Jenkins NA, Price DL, Younkin SG, Sisodia SS.** Familial Alzheimer's disease-linked presenilin 1 variants elevate Abeta1-42/1-40 ratio *in vitro* and *in vivo*. *Neuron.* 1996; 17: 1005–13.
30. **Heikkinen T, Kalesnykas G, Rissanen A, Tapiola T, Iivonen S, Wang J, Chaudhuri J, Tanila H, Miettinen R, Puolivali J.** Estrogen treatment improves spatial learning in APP + PS1 mice but does not affect beta amyloid accumulation and plaque formation. *Exp Neurol.* 2004; 187: 105–17.
31. **Wang J, Tanila H, Puolivali J, Kadish I, van Groen T.** Gender differences in the amount and deposition of amyloidbeta in APPswe and PS1 double transgenic mice. *Neurobiol Dis.* 2003; 14: 318–27.

32. **Wang L, Andersson S, Warner M, Gustafsson JA.** Estrogen receptor (ER)beta knockout mice reveal a role for ERbeta in migration of cortical neurons in the developing brain. *Proc Natl Acad Sci USA.* 2003; 100: 703–8.
33. **Fan X, Warner M, Gustafsson JA.** Estrogen receptor beta expression in the embryonic brain regulates development of calretinin-immunoreactive GABAergic interneurons. *Proc Natl Acad Sci USA.* 2006; 103: 19338–43.
34. **Yin KJ, Hsu CY, Hu XY, Chen H, Chen SW, Xu J, Lee JM.** Protein phosphatase 2A regulates bim expression via the Akt/FKHRL1 signaling pathway in amyloid-beta peptide-induced cerebrovascular endothelial cell death. *J Neurosci.* 2006; 26: 2290–9.
35. **Xie H, Clarke S.** Protein phosphatase 2A is reversibly modified by methyl esterification at its C-terminal leucine residue in bovine brain. *J Bio Chem.* 1994; 269: 1981–4.
36. **Virshup DM.** Protein phosphatase 2A: a panoply of enzymes. *Curr Opin Cell Biol.* 2000; 12: 180–5.
37. **Pei JJ, Gong CX, Iqbal K, Grundke-Iqbal I, Wu QL, Winblad B, Cowburn RF.** Subcellular distribution of protein phosphatases and abnormally phosphorylated tau in the temporal cortex from Alzheimer's disease and control brains. *J Neural Transm.* 1998; 105: 69–83.